Eur. Phys. J. D **62**, 213–217 (2011)
DOI: 10.1140/epjd/e2011-10653-y

THE EUROPEAN PHYSICAL JOURNAL D

Regular Article

The influence of the discharge parameters on the plasma spatial structuring in argon DBDs

I.A. Shkurenkov[a], Yu.A. Mankelevich, and T.V. Rakhimova

Skobeltsyn Institute of Nuclear Physics, Lomonosov's Moscow State University, Leninskie Gory, 119991 Moscow, Russia

Received 15 November 2010 / Received in final form 17 January 2011
Published online 25 March 2011 –

Abstract. The plasma parameters, discharge plasma uniformity and filamentation processes in high pressure (near atmospheric pressure) dielectric barrier discharges (DBD) in argon are studied using the developed two-dimensional 2D(r, z) model. The applied voltage frequency, the voltage shape, the dielectric layers material and its thickness are varied and the effects of such variations on plasma uniformity, discharge structure and operation are studied. The DBD discharges with different dielectric layers thickness, dielectric constants and secondary electron emission coefficients are simulated. It was shown that the dielectric layer thickness is an important parameter for producing high pressure discharges uniform over the radius. The possibility of the radially uniform discharges at atmospheric pressure was shown in the present study.

1 Introduction

Dielectric barrier discharge is a well-known method for producing homogeneous glow discharges at high pressures. The DBDs can be conveniently operated over a wide range of the discharge parameters. That is why the DBD systems have many applications, such as ozone generation, excimer UV lamps, plasma display panels [1] and in pulser-sustainer discharge systems [2]. DBDs are successfully applied to pollution control and to polymer surface treatment in order to promote wettability, printability, and adhesion [3]. The recent investigations [4,5] showed that they find various applications in the biomedical applications. Various configurations of the DBD were designed for a great number of its applications. For example, several flow control technologies have emerged recently. The actuators based on non-thermal surface plasma discharge are identified as being suitable for subsonic flow control [6,7]. The atmospheric pressure barrier discharges in noble gases with plasma propagation (outlet) in ambient air [8] are studied as a perspective plasma-processing system for various applications e.g. surface treatment, bio-medical applications etc.

However, the discharge at about atmospheric pressure falls into many independent thin current filaments [9]. The appearance of the filaments depend on the discharge parameters such as discharge feed gas, gas pressure, gas gap, dielectric surface properties and applied voltage frequency [10]. The discharge filamentation occur over a wide range of the parameters (gas pressure, frequency and amplitude of the supply power). The reasons resulting in the appearance of the current filaments were studied in [9].

Many authors distinguish between two DBD discharge modes: streamer and glow. The glow mode of DBDs is not necessarily uniform, but can be filamentary also. These glow filaments are formed by avalanches rather than streamers (microdischarges are initiated by Townsend, not a streamer breakdown) [11–13]. The DBD and its modes were the subjects of many studies in the recent years. From the large number of publications on homogeneous DBDs one can conclude that many parameters including the properties of the power supply, the dielectric barriers, the used gas and pressure, the geometrical configuration and, most strikingly, the operating frequency have an influence. Memory effects including surface charges and long living species from the previous half cycle play a dominant role [14,15]. For example, the RF DBD was studied in [16,17]. Their simulation results suggest that the formation of filaments observed in an atmospheric pressure argon discharge under RF excitation could be triggered by the regime transition $\alpha \rightarrow \gamma$.

The effect of the normal current density was obtained numerically in the filamentary DBD simulations in [9]. The nonstationarity of the boundary of the current channel results in the widening or narrowing of the current channel. The increase in the discharge current occurs due to increase in the number of rings and as a result in the discharge area expansion. The electron concentration and current density in each ring with the applied voltage increase or drop respectively tend to be the same.

The present study is the further development of the simulations [9]. The paper presents the calculated results for the high pressure (near atmospheric pressure) DBDs in

[a] e-mail: chkouren@gmail.com

argon. The influence of the discharge parameters is studied in the present paper. First, the applied voltage frequency and the voltage shape were varied. The discharge modeling results for different applied voltages and dielectric layers are presented here. The dielectric layers thickness, the dielectric constant and the secondary electron emission coefficient were varied to reveal the conditions promoting discharge uniformity.

2 2D modeling. Effects of discharge parameters variations

The detailed description of the 2D model describing spatial distributions of macroscopic plasma parameters is presented in [9,18]. This model includes the conservation equations for number densities of electrons, Ar^+ and Ar_2^+ ions, and excited atoms (in the effective metastable Ar^m, resonant Ar^r states and excimers Ar_2^*). Electric field E is calculated form Poisson's equation. The developed model was tested for two different experimental data. The comparison of the calculated results showed the good agreement with experimental ones. The basic gas pressure used in our calculations is 60 torr, but there were the calculations (discussed at the end of the article) at atmospheric pressure (760 torr).

The model scheme of the discharge is shown in Figure 1. The simulated discharge is ignited between two planar electrode disks. The simulation area consists of a gas cylindrical region ($R+R_e$, $d_g = 0.15$ mm) and two dielectric layers (with thickness $d_d = 2$ mm and permittivity $\varepsilon = 4$). The electrodes radius is $R = 2.5$ cm. To avoid the perturbations from the boundaries of the electrodes we extended the calculation region beyond the electrodes edge for extra distance $R_e = 1$ cm. So at the right side there is distance R_e between the end of the electrode and the end of the simulation area. The cell sizes in axial and radial directions are 0.0015 cm and 0.03125 cm, respectively.

The boundary conditions for the electric potential at the top and bottom borders should be discussed. The conditions in the region without electrodes are the electric potential distribution produced by the electrodes potentials. According to superposition principle the electric field between the dielectrics in the region without electrodes is determined by the potential of the electrodes without dielectrics and charges on the dielectrics and in the gas gap. As a first approximation for boundary conditions we have calculated electric field distribution in absence of the dielectrics and charged particles. These distributions are shown in Figure 1. The simulations show that such discharges are unstable against the radial disturbance. The mechanisms of the concentric rings formation, which is the first stage of the discharge filamentation process, were discussed in [9]. The brief description of this process is presented here. Several experimental and theoretical studies of the discharge filamentation [19,20] show that the discharge filamentation starts at the boundary of the initially uniform over the radius current channel. The disturbance appears at the edge of the discharge current channel, and

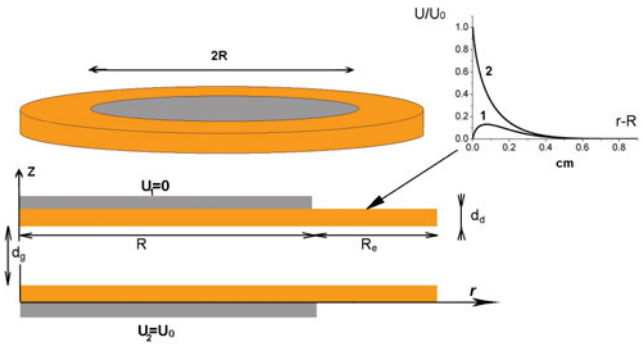

Fig. 1. (Color online) The scheme of the simulated DBD discharge. $Z = 0$ at the upper electrode (grey).

during the following breakdowns it moves from the edge to the centre and the system of the concentric rings forms. After the stage of the rings formation (about 2 periods) the rings start to fall apart into filaments (about 12 periods).

It should be taken into account that the discharge plasma produced in the result of the previous breakdown does not decay completely for the next half-period. The electrons move to the anode before the breakdown, but they are not able to reach the surface as both dielectrics surfaces are charged negatively during all the period. The anode surface is negatively charged and the electrons moving between the breakdowns are concentrated near the anode. The plasma electrons concentration near the anode and the positive plasma potential at the same time results in the appearance of the radial electron fluxes oppositely directed. This causes the appearance of the first ring at the edge with high electron concentration. The appearance of the disturbance in the near anode region and its motion to the cathode is shown in Figure 2. It must be noted that the radial electron flux during the breakdown is smaller than the axial electron flux (axial one is up to 10^{19} cm^{-2}/s). The most important thing is that the disturbance at the boundary appears near the anode and expands through all the discharge volume during the breakdown.

Figure 3 shows the appearance of the disturbance and its expansion to the center of the current channel. The appearance of such disturbance is caused by the spatial distribution of the charges in the discharge during the breakdown. It was shown in [9] that the concentric rings formation caused by the radial electric field peculiarity in the near dielectric surface region. The radial electric field is much smaller than the axial electric field ($E_r = 1000$ V, $E_z = 7000$ V in the anode layer). The non-uniform radial electric field distorts the initially uniform surface charge distribution over the radius. The non-uniform surface charge distribution increases the radial electric field and promotes the electric field peculiarity expansion to the center ($r = 0$) of the current channel. The influence of the discharge parameters variations on the plasma spatial structuring for the discharge of kilohertz range was studied and the results of this study are described below. The simulations were carried out at three different values

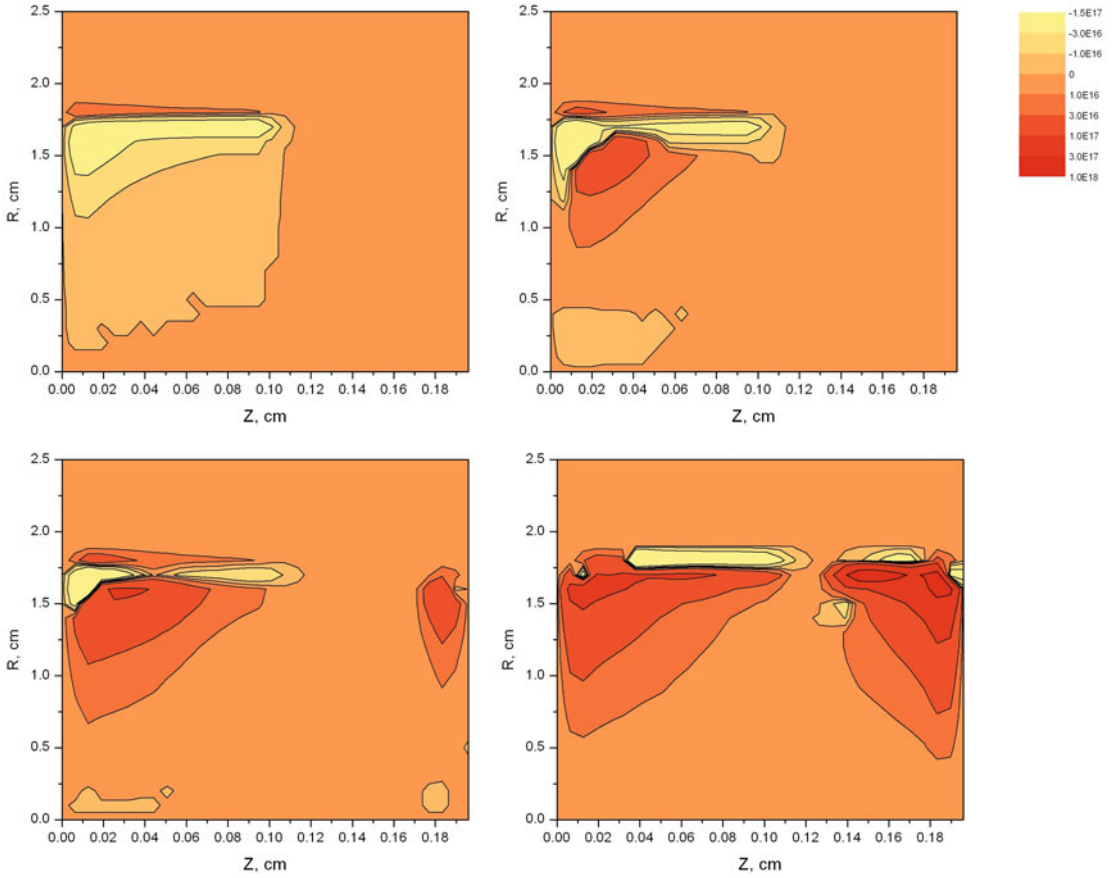

Fig. 2. (Color online) The spatial distributions of the radial electron fluxes at different moment of time during the first breakdown (3, 6, 9, 15 ns from the breakdown beginning, respectively).

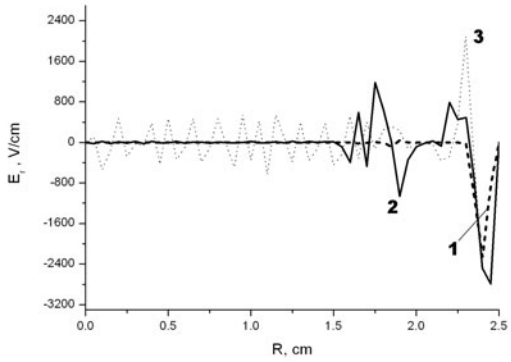

Fig. 3. The radial electric fields in the near anode region at first, second and third breakdown, respectively (in the discharge current maximum).

of the applied voltage frequencies – 45, 90 and 130 kHz. The applied voltage amplitude is 1000 V. The simulations show that the increase in the frequency leads to the more uniform discharge structure over the radius. The radial distributions of electron concentration in the discharges at different applied voltage frequencies (45 and 130 kHz) are presented in Figure 4. It is seen that the discharge at 130 kHz is uniform over the radius, while there is a periodic structure in the surface charge radial distribution in the discharge at 45 kHz. The simulations show that the discharge transition to the visibly uniform mode occurs at the frequency of about 100 kHz.

The different meanders of applied voltage are also simulated here. The applied voltage is 2000 V; the pulses are mono-polar. Pulse duration is 50 ns and repetition rate is 50 kHz. Simulations show that such discharges are uniform over the radius in this case. There is a stepwise electric field switching on (the increase of the applied voltage occur very fast) and the electrons do not concentrate near the anode before the breakdown. The electron concentration decreases between the breakdowns and the disturbance is not able to change the plasma spatial structure here.

Using the RF equipment or specific forms of applied voltage pulses is not always convenient, so the other ways producing discharge uniform over the radius is studied in the present paper. The results of the discharge simulations with different dielectric materials and thickness are reported below.

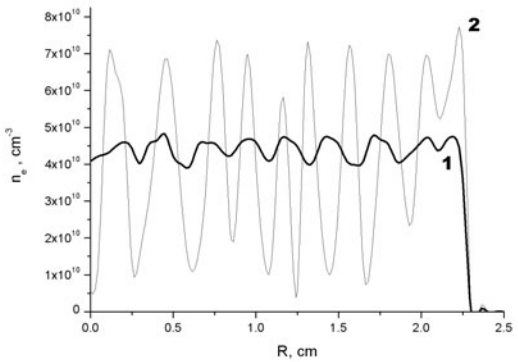

Fig. 4. The radial distributions of the electron concentration averaged over the period at different applied voltage frequencies (curve 1–130 kHz and 2–45 kHz).

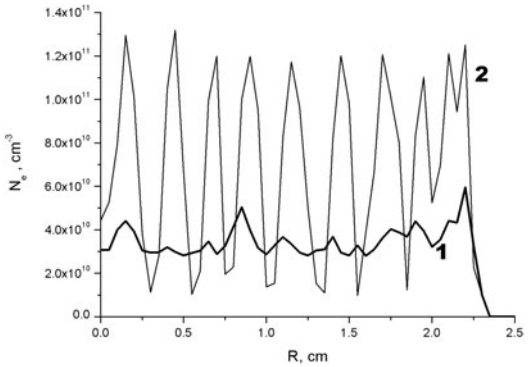

Fig. 5. The radial electron concentration distribution averaged over the period (1 – $\varepsilon = 2$, $l = 0.02$ and 2 – $\varepsilon = 10$, $l = 0.1$).

We have also studied the influence of the secondary electron emission coefficient variation on the discharge radial structure. The simulated discharge is operated in α-mode. The secondary electrons emitted from the dielectric surface as a result of ion impacts do not influence significantly the plasma ionization. The simulations show that the secondary electrons influence a bit the discharge plasma radial structure. The secondary electron emission coefficient is 0.01 in our basic calculations. The increase in this coefficient does not influence the plasma ionization, but it leads in the more uniform discharge structure. The calculations at four different values of the secondary electron emission coefficient (0, 0.01, 0.05, and 0.1) were carried out. The discharge with secondary electron emission coefficient of 0.1 is more uniform than the others, but the further increase in γ results in the appearance of the filaments with very high electron concentration (much higher than for the case of $\gamma = 0$). The number of such filaments for $\gamma = 0.1$ is less than for $\gamma = 0.01$. So, there is some kind of optimum value. It should be noted here, that the variation of γ does not influence seriously the plasma spatial structure. It is not possible to obtain the discharge uniform over the radius at atmospheric pressure. The described above effects of γ variation were observed in the discharges at pressure of about 40–80 torr. The effect of γ variation is weak at higher pressures.

It is well known that the discharge plasma parameters depend on the ε/l parameter. Here, ε is the dielectric constant and l is the dielectric layer thickness. The surface charge value and electric field depend on this parameter. So the thick dielectric layer with high ε value is similar to the thin layer with low permittivity in this sense. However, our calculations show although that the plasma radial structure depends more on l that on ε. Figure 5 presents the radial electron concentration distribution averaged over the period in the discharges with $\varepsilon = 2$, $l = 0.02$ and $\varepsilon = 10$, $l = 0.1$, respectively. The ratio ε/l is the same in both cases but the discharge is more uniform in the first case. The voltage drop and longitudinal electric field depend only on the ε/l parameter, but the

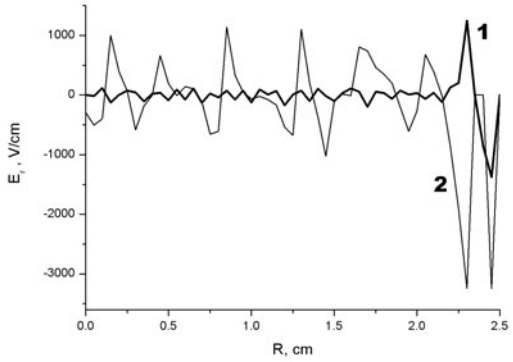

Fig. 6. The radial distributions of the radial electric field (1 – $\varepsilon = 2$, $l = 0.02$ and 2 – $\varepsilon = 10$, $l = 0.1$).

radial electric field depends also on the dielectric layer thickness. Figure 6 presents the radial distributions of the radial electric field in both cases. Boundary region is on the right side ($R = 2.5$ cm). It is seen that there is a high peak of the radial electric field in the boundary region in both cases, but the internal regions differ a lot. There are high peaks in the discharge with thick dielectric layer, while the electric field radial distribution is much more uniform in the discharge with thin dielectric layer. The radial electric field disturbance does not expand in the internal region when the thin dielectric layer is used.

The DBDs properties (the current self-restriction) remain even when the thin dielectric is used. The discharge filamentation is the result of the near-anode instability toward the radial disturbances [21]. The anode layer is more stable toward such disturbances when the thin dielectric is used and radial disturbances of the potential distribution are depressed. Thus the more uniform discharges (over the radius) could be produced by using thin dielectric layers. One may use also the materials with high relative permittivity (high-k materials) to reinforce the effect. The calculations were carried out to study the possibility of

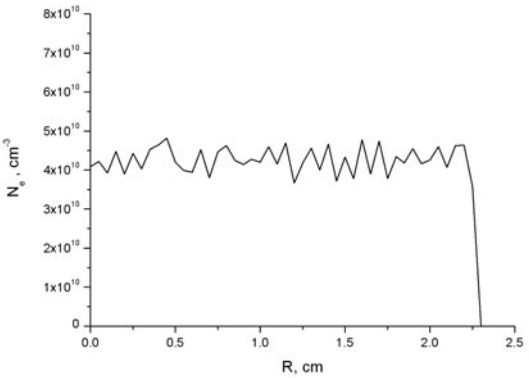

Fig. 7. The radial distribution of electron concentration averaged over the period in the atmospheric pressure discharge ($\varepsilon = 15$, $l = 0.005$ cm).

the uniform discharges production at atmospheric pressure. Figure 7 presents the radial distribution of electron concentration averaged over the period in the atmospheric pressure discharge. The peaks of the electron concentration are not very high here and they can not be observable by the eye in the experiments. One may conclude that it is an example of the uniform discharge at atmospheric pressure. The discharge is operated under the following conditions: the dielectric layer thickness is 0.05 mm; the dielectric constant is 15, the secondary electron emission coefficient is 0.05 and the applied voltage frequency is 45 kHz. This discharge is close to the uniform, but this prediction requires the experimental verification. The electric field in the dielectric is about 12 MV/m. That is very high electric field, but there are some materials, such as hafnium dioxide (HfO_2), that can stand the high fields and realize the required conditions. So the DBDs at atmospheric pressure may be produced by using appropriate materials.

3 Conclusions

The 2D model developed in our previous study [9] is used here for the simulation of high pressure (near atmospheric pressure) DBDs, it's uniformity and operation in argon. The influence of the discharge parameters is studied here. First, the applied voltage frequency and the voltage shape were varied. The simulations show that the discharges at higher applied voltage frequencies are more uniform over the radius. The discharge with meander applied voltage is uniform at high pressures. The DBD discharges with different dielectric layers are simulated. The dielectric layers thickness, the relative dielectric permittivity and the secondary electron emission coefficient were varied. The secondary electron emission does not affect seriously the discharge plasma, but the simulations show that the increase of the secondary electron emission coefficient up to $\gamma = 0.1$ results in more uniform discharge plasma distribution. The further increase of γ leads to the degradation of the discharge uniformity. It was shown that the thin dielectric layers with high dielectric constants promote the uniformity of high pressure DBDs. The possibility of the discharges uniform over the radius production at atmospheric pressure was shown in the present study.

This study is carried out in the frame of Russian Government Grant (02.740.11.5108) and Key Science School Grant (SS-3322.2010.2).

References

1. U. Kogelschatz, Plasma Chem. Plasma Process. **23**, 0272 (2003)
2. J.R. Bruzzese, A. Hicks, A. Erofeev, A.C. Cole, M. Nishihara, I.V. Adamovich, J. Phys. D **43**, 015201 (2010)
3. A. Chirokov, A. Gutsol, A. Fridman, Pure Appl. Chem. **77**, 487 (2005)
4. M. Laroussi, IEEE Trans. Plasma Sci. **37**, 0093 (2009)
5. G. Fridman, A. Shereshevsky, M.M. Jost, A.D. Brooks, A. Fridman, A. Gutsol, V. Vasilets, G. Friedman, Plasma Chem. Plasma Process. **27**, 163 (2007)
6. N. Benard, A. Mizuno, E. Moreau, J. Phys. D **42**, 235204 (2009)
7. D.F. Opaits, M.N. Shneider, R.B. Miles, A.V. Likhanskii, S.O. Macheret, Phys. Plasma **15**, 073505 (2008)
8. Q. Li, X.M. Zhu, J.T. Li, Y.K. Pu, J. Appl. Phys. **107**, 043304 (2010)
9. I.A. Shkurenkov, Y.A. Mankelevich, T.V. Rakhimova, Eur. Phys. J. D **61**, 95 (2011)
10. U.N. Pal et al., J. Phys. D **42**, 045213 (2009)
11. I. Brauer, C. Punset, H.G. Purwins, J.P. Boeuf, J. Appl. Phys. **85**, 7569 (1999)
12. I. Muller, C. Punset, E. Ammelt, H.G. Purwins, J.P. Boeuf, IEEE Trans. Plasma Sci. **27**, 20 (1999)
13. A. Chirokov, A. Gutsol, A. Fridman, Pure Appl. Chem. **77**, 487 (2005)
14. U. Kogelschatz, J. Phys. Conf. Ser. **257**, 012015 (2010)
15. P. Zhang, U. Kortshagen, J. Phys. D **39**, 153 (2006)
16. N. Balcon, A. Aanesland, R. Boswell, Plasma Source. Sci. Technol. **16**, 217 (2007)
17. N. Balcon, G.J.M. Hagelaar, J.P. Boeuf, IEEE Trans. Plasma Sci. **36**, 2782 (2008)
18. I.A. Shkurenkov, Y.A. Mankelevich, T.V. Rakhimova, Phys. Rev. E **79**, 046406 (2009)
19. L. Stollenwerk, S. Amiranashvili, J.P. Boeuf, H.G. Purwins, Eur. Phys. J. D **44**, 133 (2007)
20. L. Stollenwerk, S. Amiranashvili, J.P. Boeuf, H.G. Purwins, Phys. Rev. Lett. **96**, 255001 (2006)
21. Y.S. Akishev, A.M. Volchek, A.P. Napartovich, N.I. Trushkin, Plasma Source. Sci. Technol. **1**, 190 (1992)